

INFLUENCE OF NOISE-INDUCED MODULATIONS ON THE TIMING STABILITY OF PASSIVELY MODE-LOCKED SEMICONDUCTOR LASER SUBJECT TO OPTICAL FEEDBACK

LINA JAURIGUE ¹ and KATHY LÜDGE ¹

(Received 15 October, 2024; accepted 28 February, 2025)

Abstract

We show that passively mode-locked lasers, subject to feedback from a single external cavity can exhibit large timing fluctuations on short time scales, despite having a relatively small long-term timing jitter. This means that the commonly used von Linde and Kéfélian techniques of experimentally estimating the timing jitter can lead to large errors in the estimation of the arrival time of pulses. We also show that adding a second feedback cavity of the appropriate length can significantly suppress noise-induced modulations that are present in the single feedback system. This reduces the short time-scale fluctuations of the interspike interval time and, at the same time, improves the variance of the fluctuation of the pulse arrival times on long time scales.

2020 Mathematics subject classification: primary 00A71; secondary 00A72, 00A79.

Keywords and phrases: mode locking, timing jitter, delay differential equation.

1. Introduction

Passively mode-locked semiconductor lasers are envisaged as a compact, inexpensive alternative to other pulsed sources of light [6, 27, 31, 41]. However, for this to be realized, the issue of their relatively large timing jitter needs to be overcome. To this end, research has been carried out on various techniques of improving the timing regularity of such devices. These techniques include hybrid mode-locking [2, 15], optical injection [14, 42, 43], opto-electronic feedback [13] and optical feedback [3–5, 7, 9, 10, 12, 23, 28, 29, 36, 37, 46, 47, 52, 53]. All-optical feedback has been of particular interest, as this technique is very simple to implement and does not require any additional electronics. Theoretical studies on this topic have predicted

¹Institute of Physics, Technische Universität Ilmenau, Weimarer Straße 25, 98693 Ilmenau, Germany; e-mail: lina.jaurigue@tu-ilmenau.de, kathy.luedge@tu-ilmenau.de

© The Author(s), 2025. Published by Cambridge University Press on behalf of Australian Mathematical Publishing Association Inc.

that a reduction in the timing jitter can be achieved when resonant feedback lengths are chosen, that is, integer multiples of the period of the laser [34, 37], and that better reduction can be achieved for longer delay times [23]. Experimentally, a resonance structure in dependence on the delay length has also been observed, as well as improved timing jitter reduction for longer feedback cavities [3, 4, 29, 33]. However, for longer delay times, the influence of noise-induced modulations plays an increasingly important role. These modulations are seen experimentally as side peaks in the power spectra of the laser output, and are sometimes referred to as supermode resonances. So far, there appears to be a lack of understanding of how these noise-induced modulations affect the timing regularity of passive mode-locking lasers [5, 9, 10, 12, 19, 52, 53]. In this paper, we will show how noise-induced modulations affect the pulse train and how this influences the common measures of the timing jitter.

Noise-induced oscillations (the underlying deterministic system is in a steady state) or modulations (the underlying deterministic system exhibits oscillatory dynamics) have been studied and observed in a wide range of systems [8, 18, 24, 40, 45, 55]. There have also been several works on the suppression thereof, particularly using feedback [16, 19, 22, 24, 40]. In this paper, we will show how the timing regularity of the mode-locked laser output can be improved by implementing a dual feedback cavity configuration, where the second cavity acts to suppress the noise-induced modulations arising due to the first feedback cavity.

The paper is structured as follows. In Sections 2.1 and 2.2, we present the model for the passively mode-locked laser subject to optical feedback and various methods of determining long-term timing jitter. In Section 3.1, we look at the influence of resonant optical feedback from one external cavity on the regularity of the pulse train and demonstrate the impact of noise-induced modulations. In Section 3.2, we propose a simplified iterative map that can reproduce the effect of the modulations. Subsequently, in Section 3.3, we show that the noise-induced modulations can be suppressed via the addition of a second feedback cavity with an appropriately chosen length and we identify optimal conditions for the second feedback cavity to achieve both modulation suppression and low long-term timing jitter. Finally, we discuss the results and conclude.

2. Methods

2.1. Delay differential equation model We use the model presented in [22] for a two-section passively mode-locked semiconductor laser, subject to optical feedback from two external cavities (a sketch of the setup is shown in Figure 1(a)). The model is based on that proposed in [48–50], which was extended to include optical feedback in [37]. The laser is described by a set of three delay differential equations:

$$\begin{aligned} \dot{\mathcal{E}}(t) = & -\gamma\mathcal{E}(t) + \gamma R(t-T)e^{-i\Delta\Omega T}\mathcal{E}(t-T) + \sqrt{R_{sp}}\xi(t) \\ & + \sum_{l=1,2} K_l e^{iC_l} \gamma R(t-T-l\tau_l) e^{-i\Delta\Omega(T+l\tau_l)} \mathcal{E}(t-T-l\tau_l), \end{aligned} \quad (2.1)$$

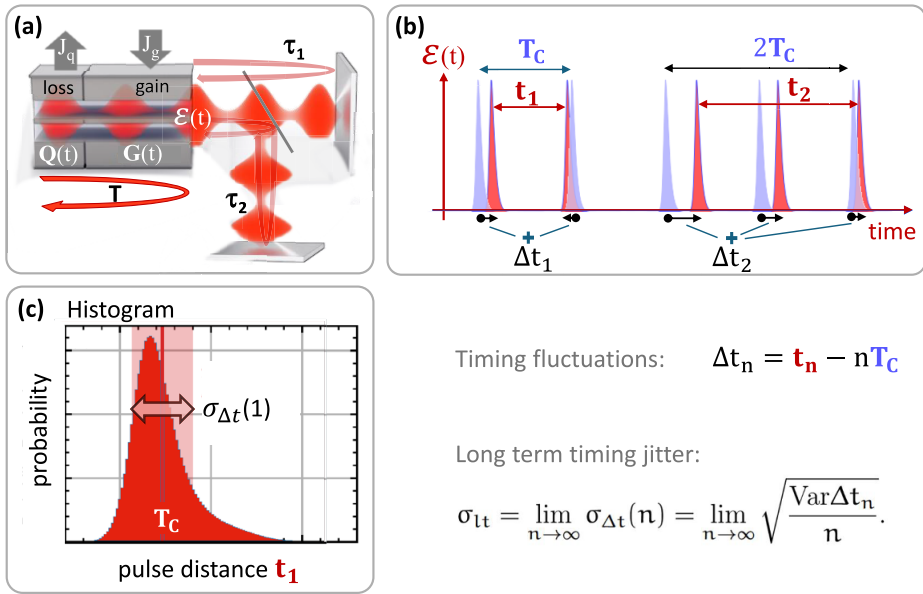


FIGURE 1. (a) Sketch of the two-section passively mode-locked laser with two external feedback cavities explaining the quantities in the delay differential equation model (2.1)–(2.3). (b) Sketch of the emitted pulse train in red, blue pulses represent idealized pulses with equal distance T_C (T_C is the mean pulse distance), arrows indicate definition of timing fluctuations Δt_n . (c) Visualization of the distribution of pulse intervals t_1 , pulse-to-pulse timing jitter is $\sigma_{pp} = \sigma_{\Delta t}(n = 1)$, long-term jitter is defined as $\sigma_{lt} = \sigma_{\Delta t}(n \rightarrow \infty)$.

Timing fluctuations: $\Delta t_n = t_n - nT_C$

Long term timing jitter:

$$\sigma_{lt} = \lim_{n \rightarrow \infty} \sigma_{\Delta t}(n) = \lim_{n \rightarrow \infty} \sqrt{\frac{\text{Var} \Delta t_n}{n}}$$

$$\dot{G}(t) = J_g - \gamma_g G(t) - e^{-Q(t)}(e^{G(t)} - 1)|\mathcal{E}(t)|^2, \tag{2.2}$$

$$\dot{Q}(t) = J_q - \gamma_q Q(t) - r_s e^{-Q(t)}(e^{Q(t)} - 1)|\mathcal{E}(t)|^2, \tag{2.3}$$

with

$$R(t) \equiv \sqrt{\kappa} e^{1/2((1-i\alpha_g)G(t) - (1-i\alpha_q)Q(t))}$$

being the change of the slowly varying electric field amplitude \mathcal{E} during one roundtrip in the ring cavity (α_g, α_q are the linewidth enhancement factors in the gain and absorber sections which we assume to be zero [20]). All transmission, coupling and internal losses at the interfaces between the different sections are lumped together into the attenuation factor κ .

The saturable gain G and the saturable loss Q are effective dynamic variables that describe dimensionless carrier densities. They have been obtained from the travelling wave model via integration of the carrier densities within the gain and absorber sections [37]. The same holds true for the pump parameters J_g and J_q , which are integrated and rescaled values that are proportional to the injection current in the gain

TABLE 1. Parameter values used in numerical simulations, unless stated otherwise.

Parameter	Value	Parameter	Value	Parameter	Value
γ	2.66 ps^{-1}	κ	0.1	T	25 ps
γ_g	1 ns^{-1}	α_g	0	R_{sp}	0.04 ps^{-1}
γ_q	75 ns^{-1}	α_q	0	C_1	0
J_g	0.12 ps^{-1}	r_s	25	C_2	0
J_q	0.3 ps^{-1}	$\Delta\Omega$	0	T_0	25.373 ps

section and to reverse bias induced carrier losses in the absorber section [37]. The carrier decay rates inside the gain and absorber sections are denoted by γ_g and γ_q , respectively (for semiconductor materials, the lifetime of carriers within the gain γ_g is much smaller than in the absorber γ_q [1]).

The finite width of the gain spectrum is taken into account by a bandwidth-limiting element, which is described by a Lorentzian-shaped filter function with a width of γ . If the gain is centred at the optical frequency of the closest cavity mode (assumed here for simplicity), the detuning $\Delta\Omega$ is zero. Inhomogeneous broadening is not taken into account here, but could also be included in the model [39]. The last terms in (2.2) and (2.3) describe the light–matter interactions which leads to a depletion by the pulse that travels in the cavity. The factor r_s is proportional to the ratio of the linear gain coefficients of the absorber and gain sections. Spontaneous emission noise is taken into account in (2.1) via a complex Gaussian white noise term $\xi(t)$ with a strength $\sqrt{R_{sp}}$, where R_{sp} is the spontaneous emission rate. All laser parameters are as described in [22] and given in Table 1, and correspond to parameters that model the experimentally observed emission of semiconductor-based two-section passively mode-locked lasers [33].

Here, K_1 and K_2 are the feedback strengths from the two external cavities with delay lengths τ_1 and τ_2 , respectively. Under the assumption of weak feedback, we only include contributions to the feedback from light that has made one roundtrip in the feedback cavities [37]. Here, C_1 and C_2 are the phase shifts accumulated after one roundtrip in the external cavities.

Feedback influences the dynamics of the mode-locked laser [34, 35]; however, in this paper, we are primarily interested in the reduction of the timing jitter for fundamental mode-locking, so we therefore restrict our study to only resonant feedback delay times, that is, integer multiples of the mode-locked pulse period which we denote as T_0 . Note that due to the light–matter interaction within the cavity, the period of the deterministic solution T_0 is slightly larger than the cold cavity roundtrip time T . Additionally, we set the feedback phases C_l to zero, as these have no qualitative influence on the timing jitter reduction trends in dependence of the feedback delay lengths [22, 37]. When we discuss single-cavity feedback ($K_2 = 0$), we will refer to the feedback strength K and delay length τ . In the following, the parameter values used

will be those given in Table 1, unless stated otherwise. The laser cavity roundtrip used here, $T = 25$ ps, corresponds to a 1 mm Fabry–Perot cavity [35].

2.2. Timing jitter calculation methods For passively mode-locked lasers, there are several measures of the timing jitter that are commonly used. Experimentally, the so called root mean square (r.m.s.) timing jitter is usually calculated using the von Linde method [51], which involves integrating over the side band of a peak in the power spectrum of the laser output, or the timing jitter is calculated via the Kéfélian method from the width of the fundamental peak in the power spectrum [25]. This is commonly used in experimental studies [10, 12, 13, 25, 53]. For our numerical calculations, it is more convenient to derive the *long-term timing jitter* directly from the timing fluctuations [26, 36]. Please see Figure 1(b) for a visualization of their definition. We will compare this approach also with the power spectrum based Kéfélian method. In the following, we present the three methods that are used in this study to calculate the timing jitter.

(1) The Kéfélian method [25] assumes a Lorentzian line shape of the peaks in the power spectrum and gives the *long-term timing jitter* $\sigma_{lt}(h)$ as a function of the number of the harmonic h by

$$\sigma_{lt}(h) = T_C \sqrt{\frac{\Delta\nu_h T_C}{2\pi h^2}}, \quad (2.4)$$

where $\Delta\nu_h$ is the width of the Lorentzian fitted to the h th harmonic of the power spectral density of the laser output $|E|^2$ and T_C is the mean pulse period. Note that the quantity defined by (2.4) is also sometimes referred to as the *pulse-to-pulse jitter* [12, 25] which, however, rather describes the width of the inter-pulse distance distribution (see Figure 1(c) for a visualization).

(2) The timing jitter can also be calculated directly from the pulse arrival times [26, 36]. Defining timing fluctuations as shown in Figure 1(b) by

$$\Delta t_n \equiv t_n - nT_C,$$

where t_n is the arrival time of the n th pulse and nT_C is the “ideal” arrival time of the n th pulse in the jitter free case, the *long-term timing jitter* is given by

$$\sigma_{lt} = \lim_{n \rightarrow \infty} \sigma_{\Delta t}(n) = \lim_{n \rightarrow \infty} \sqrt{\frac{\text{Var}\Delta t_n}{n}}. \quad (2.5)$$

As a passively mode-locked laser does not have a clock time, T_C is the average interspike interval time calculated over many noise realizations (experimental runs). We calculate the timing fluctuations and the variance $\text{Var}\Delta t_n$ thereof by detecting the pulse positions t_n in a long train of emitted pulses as described in [36]. It is noted that there are also other very efficient methods for timing jitter calculation as published by Meinecke et al. [32]; however, for our case with side modes, they are not suitable.

(3) For numerical simulations of passively mode-locked lasers with optical feedback, there is also a semi-analytic method of calculating the *long-term timing jitter*

[23, 38]. In [23], the following expression was derived from the semi-analytic timing jitter for resonant feedback delay lengths $\tau = qT_C$, $q \in \mathbb{N}$:

$$\sigma_{t_l}(q) = \frac{\sigma_{t_l}^{\tau=0}}{1 + qK\mathcal{F}(K)}. \quad (2.6)$$

Here, $\sigma_{t_l}^{\tau=0}$ is the timing jitter for instantaneous feedback ($\tau = 0$) and $\mathcal{F}(K)$ a semi-analytic expression depending on the laser parameters and feedback strength and must be calculated numerically, as described in [23]. Equation (2.6) holds for sufficiently small noise terms in (2.1)–(2.3) and as long as all non-neutral eigenmodes of (2.1)–(2.3), linearized about the mode-locked solution, have eigenvalues λ with $\text{Re}\lambda \ll 0$, that is, as long as the influence of noise-induced modulation can be neglected.

3. Results

3.1. Timing jitter in passively mode-locked lasers subject to optical feedback from one external cavity In the limit that the timing fluctuations behave like a random walk, all the measures of the timing jitter described in Section 2.2 are directly proportional to one another [23, 36]. For a solitary laser, this limit is reached when one considers the timing fluctuations over time spans that are much longer than any internal time scales that exist in the laser system. The solitary laser pulse positions are correlated over a few roundtrips in the laser cavity due to the finite time the system requires to recover from perturbations and thus the internal time scale is determined by the relaxation oscillation frequency. This means that on time scales of a few thousand laser cavity roundtrips, the timing fluctuations behave like a random walk, meaning that the variance of the timing fluctuations grows linearly with the number of roundtrips [23, 36].

By adding optical feedback to a passively mode-locked laser, an additional time scale is introduced to the system, which has two major effects. First, the pulse positions become correlated over the delay time of the feedback cavity, which leads to a reduction in the timing jitter. This was shown in [23] using a semi-analytic approach to calculate the long-term timing jitter. Second, the stability of the mode-locked solution is decreased, which can lead to noise-induced modulations with frequencies related to the feedback delay time [24, 54]. We will now look at the consequences of these two effects.

In Figure 2(a), the power spectrum of the simulated mode-locked laser without feedback is shown at the fundamental frequency (first harmonic), while the inset shows the full spectrum. Figure 2(b) shows the timing jitter $\sigma_{\Delta t}(n)$ determined from the timing fluctuations Δt_n as a function of the roundtrip number n (defined in (3.1)),

$$\sigma_{\Delta t}(n) = \sqrt{\frac{\text{Var}\Delta t_n}{n}}. \quad (3.1)$$

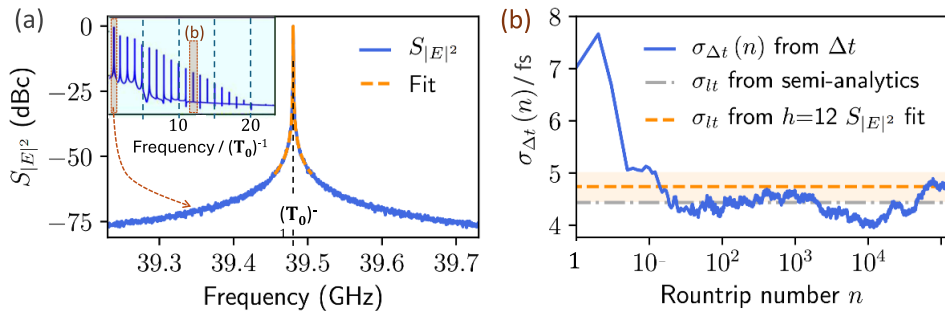


FIGURE 2. Spectra and timing jitter without delay. (a) Zoom of first peak of the electric field power spectrum $S_{|E|^2}$ (blue) with a Lorentzian line shape fitted to the first harmonic peak (orange, dashed), inset shows full power spectrum, T_0 is the mode-locking period. (b) Normalized standard deviation of the pulse arrival times $\sigma_{\Delta t}(n)$, (3.1), as a function laser cavity roundtrip number (blue). Grey dash-dotted and orange dashed line depict timing jitter obtained via semi-analytic method ((2.6) with $\sigma_{it}^{\tau=0} = 4.4$ fs, $\mathcal{F}(K) = 0.9$) and Kéfélian method ((2.4), $h = 12$, error range shaded in orange), respectively.

For n much longer than the time scales of the dynamics of the mode-locked laser, the jitter $\sigma_{\Delta t}(n)$ determined by (3.1) converges to the long-term jitter given by (2.5) and there is an agreement with all three methods used here, that is, the timing fluctuations described by (2.5) (blue line in Figure 2(b)), the *long-term timing jitter* calculated semi-analytically using (2.6) (grey dash-dotted line), and the *long-term timing jitter* described by the Kéfélian method and calculated using (2.4) with $h = 12$ (orange dashed line).

When resonant feedback is introduced, the linewidth of the fundamental peak is reduced and supermodes start to appear in the power spectrum (the frequency spacing is given by $\approx 1/\tau$). Examples of experimentally observed noise peaks are found in [3, 9, 47]. Figure 3(a) shows example spectra for single cavity feedback with delay times of $\tau = 100T_0$ and $\tau = 1000T_0$, where T_0 is the period of the underlying deterministic system. We only consider resonant feedback and thus only delay times that are integer multiples of the natural pulse repetition frequency $1/T_0$. For non-resonant feedback conditions, complex emission dynamics is observed which is, however, not the focus of this work and so is studied in more detail elsewhere [21, 30, 44].

The timing jitter $\sigma_{\Delta t}(n)$ that results from the timing fluctuations is depicted in Figure 4 with blue lines. The long-term timing jitter calculated via the Kéfélian method ((2.4) and orange dashed lines in Figure 4) was obtained by fitting the 60th harmonic of the power spectrum (Figure 3(b)). Due to the linewidth reduction with the resonant feedback, it was necessary to fit the Lorentzian to a high harmonic such that the frequency resolution allowed for a sufficiently accurate fit.

Comparing the jitter curves of the two delays in Figures 4(a1) and 4(b1), it is apparent that for $\tau = 100T_0$, the jitter $\sigma_{\Delta t}$ converges to a constant value in much fewer roundtrips than for $\tau = 1000T_0$. This is a consequence of the pulse positions being

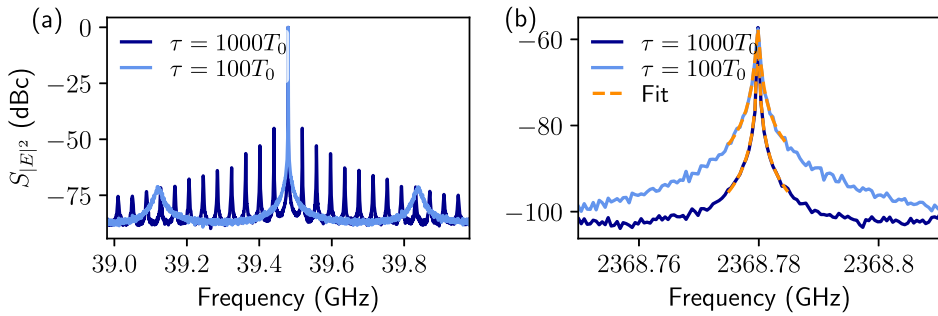


FIGURE 3. Delay-induced side modes. Power spectra $S_{|E|^2}$ of the electric field intensity for delay values of $\tau = 100T_0$ (light blue) and $\tau = 1000T_0$ (dark blue). (a) Zoom around first harmonics, (b) zoom around the central peak of the 60th harmonics with the Lorentzian fit indicated in orange.

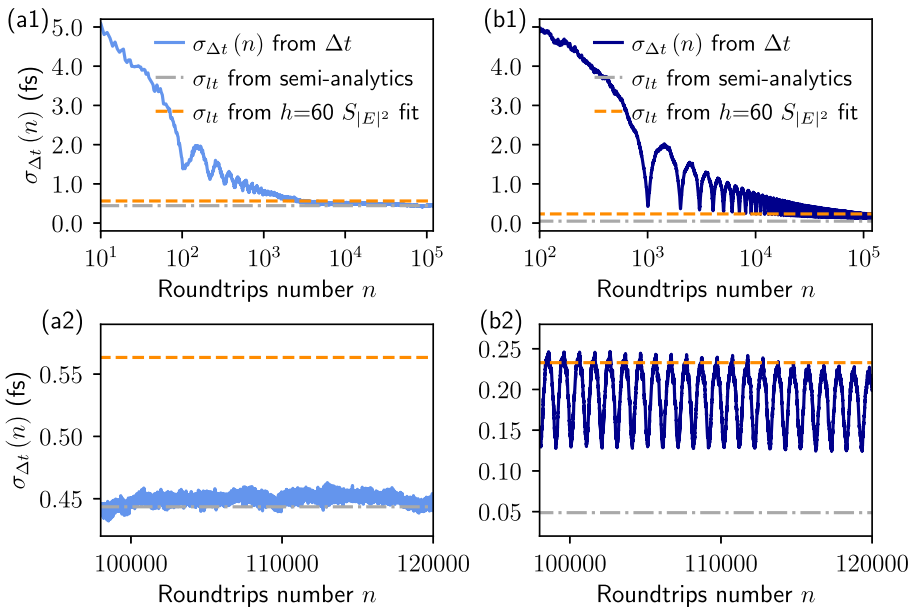


FIGURE 4. Timing jitter of mode-locked laser with one delay. Normalized standard deviation of the pulse arrival times $\sigma_{\Delta t}(n)$ as a function of the laser cavity roundtrip number n (blue lines). Grey and orange dotted lines indicate timing jitter obtained via the semi-analytic method ($\sigma_{lt}^{\tau=0} = 4.4$ fs, $\mathcal{F}(K) = 0.9$) and the Kéfélian method ($h = 60$) analogous to Figure 2 for two different delay values: (a) $\tau = 100T_0$ and (b) $\tau = 1000T_0$. Panels (a2) and (b2) are zooms of panels (a1) and (b1). Parameters: $K = 0.1$, all other parameters as in Table 1.

correlated over longer times in the longer delay case. Further, the jitter plots for the long delay show clear evidence of noise-induced modulation of the pulse arrival times. In the $\tau = 1000T_0$ case in Figure 4(b1), pronounced fluctuations in $\sigma_{\Delta t}$ are present as can be seen by the oscillating blue curve. These fluctuations have a period roughly

equal to τ and are caused by noise-induced modulations (as was also visible in the power spectra in Figure 3(a)). Noise-induced modulations are also present for smaller delay times; however, the effect is not as pronounced since the damping rate scales with $1/\tau$. The presence of the fluctuations for $\tau = 1000T_0$ means that $\sigma_{\Delta t}$ never truly converges to a constant value.

The above observations have several consequences. First, it means that the timing fluctuations are not wide-sense stationary [11], which means that one can not use the Wiener–Khinchin theorem [17] to relate the autocorrelation function of the timing deviations to the phase noise spectrum [34]. Second, in a strict sense, the long-term timing jitter cannot be calculated reliably when fluctuations are present and the long-term timing jitter calculated from the power spectrum cannot be interpreted as the variance of the timing deviations. Furthermore, the lower limit of the jitter $\sigma_{\Delta t}$ does not reach the semi-analytic limit (dash-dotted grey line in Figure 4(b2)). Whereas, for $\tau = 100T_0$, random-walk-like behaviour is regained in the jitter $\sigma_{\Delta t}(n)$ after approximately 10^4 laser cavity roundtrips and the semi-analytic limit (dash-dotted grey line in Figure 4(a2)) is reached.

We have established that the noise-induced oscillation increase the variance of the timing fluctuations (that is, the standard deviation of timing fluctuations $\sigma(\Delta t_n) = \sqrt{\text{Var}\Delta t_n}$). In addition to this, the more direct effect is that they cause periodic modulations in the timing fluctuations. An example of this is shown in Figure 5, where the timing fluctuations Δt_n are depicted for one noise realization as a function of the roundtrip number for $\tau = 1000T_0$ (in panel (a)) and $\tau = 100T_0$ (in panel (b)). If the amplitude of these delay induced modulations is sufficiently large, then the pulse arrival times can deviate significantly from the expected arrival time interval based on the long-term jitter. To illustrate this, we calculate the expected normalized standard deviation of the pulse arrivals times $\sigma(\Delta t_n)$ after 10^4 laser cavity roundtrips from the long-term timing jitter and compare this with the amplitude of the timing fluctuations depicted in Figure 5. For $\tau = 100T_0$, the long-term timing jitter is $\sigma_{lt} \approx 0.44$ fs (see Figure 4(a2)). After 10^4 roundtrips, this corresponds to a standard deviation of $\sigma(\Delta t_n) = \sigma_{lt}\sqrt{n} = 44$ fs, which dominates the amplitude of the timing fluctuations Δt_n while the delay-induced amplitudes are ≈ 40 fs in Figure 5(b). To make the same comparison for the $\tau = 1000T_0$ case, we take the value to which the minima of $\sigma_{\Delta t}$ converge, that is, a long-term timing jitter of $\sigma_{lt} \approx 0.13$ fs, as seen in Figure 4(b2). In this case, the standard deviation after 10^4 roundtrips is $\sigma(\Delta t_n) = \sigma_{lt}\sqrt{n} = 13$ fs, which is an order of magnitude smaller than the amplitude of the modulation of Δt_n shown in Figure 5(a) (≈ 130 fs).

We can thus conclude that the long-term timing jitter gives an estimate of the underlying random walk-like behaviour, but contains no information on timing deviations on short time scales. For long feedback delay times, the amplitude of the noise-induced modulations of the timing deviations can be larger than the underlying drift in the timing fluctuations, even on relatively long time scales (10^5 roundtrips corresponds to approximately 2.5 ms). Therefore, neglecting the influence of the noise-induced oscillation can lead to significant errors in the estimation of pulse arrival times.

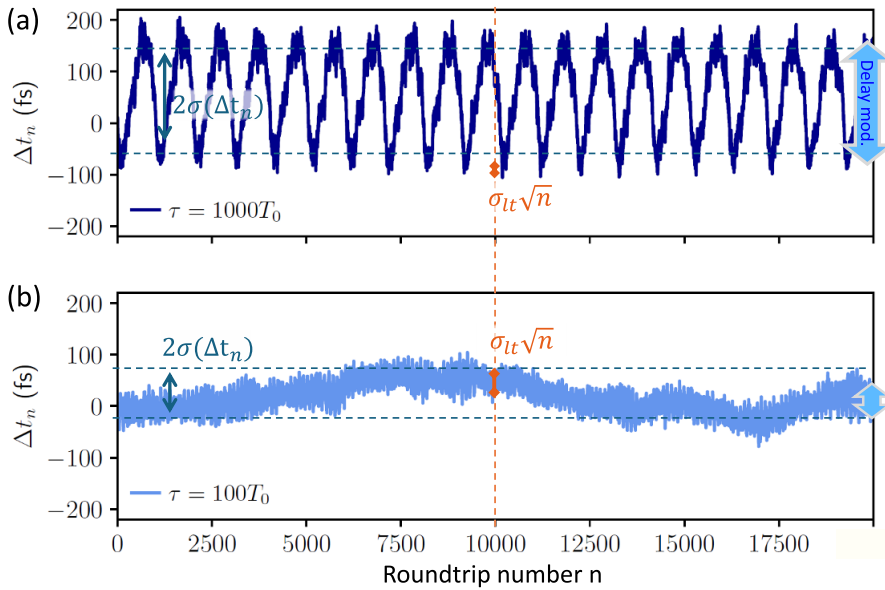


FIGURE 5. Timing fluctuations Δt_n as a function of the roundtrip number n for (a) $\tau = 1000T_0$ and (b) $\tau = 100T_0$. Delay-induced fluctuations with amplitudes of ≈ 130 fs (blue arrow on the right) dominate $\sigma(\Delta t_n)_{\tau=1000} = 78$ fs for $\tau = 1000T_0$ while they have smaller amplitudes of ≈ 40 fs for $\tau = 100T_0$ where stochastic fluctuations dominate $\sigma(\Delta t_n)_{\tau=100} = 30$ fs. Orange arrows indicate value for $\sigma_{\Delta t}(10^4)$ obtained from long-term jitter (13 fs, 44 fs). Parameters: $K = 0.1$, all other parameters as in Table 1.

3.2. Timing jitter for a driven iterative map To understand how the noise-induced modulations affect the variance of the timing fluctuations, it is helpful to consider a simple iterative map describing a random process with an added oscillatory term. We consider

$$T_{n+1} = T_n + T_P + \xi(n + 1) + a\mathcal{H}, \tag{3.2}$$

where T_P is the unperturbed inter pulse distance, $\xi(n)$ is a Gaussian white noise term and \mathcal{H} is a sinusoidal function of either the roundtrip number n or the interspike interval T_n , that is, $\mathcal{H}(n) = \sin(2\pi n/\tau_s)$ or $\mathcal{H}(T_n) = \sin(2\pi T_n/\tau_s)$, with amplitude a . If $a = 0$, then

$$T_n = nT_P + \sum_{i=1}^n \xi(i) \tag{3.3}$$

and the series $\{T_n - nT_P\}$ is a random walk. In this case, apart from statistical fluctuations, $\sigma_{\Delta t}(n)$ is constant (Figure 6, black line). If a is non-zero and $\mathcal{H}(n) = \sin(2\pi n/\tau_s)$ is used, then the sinusoidal term adds regular modulations onto the variance. For n equal to integer multiples of half the period of the modulations, τ_s , the modulations cancel and $\sigma_{\Delta t}(n)$ is the same as in the $a = 0$ case (compare red and black line

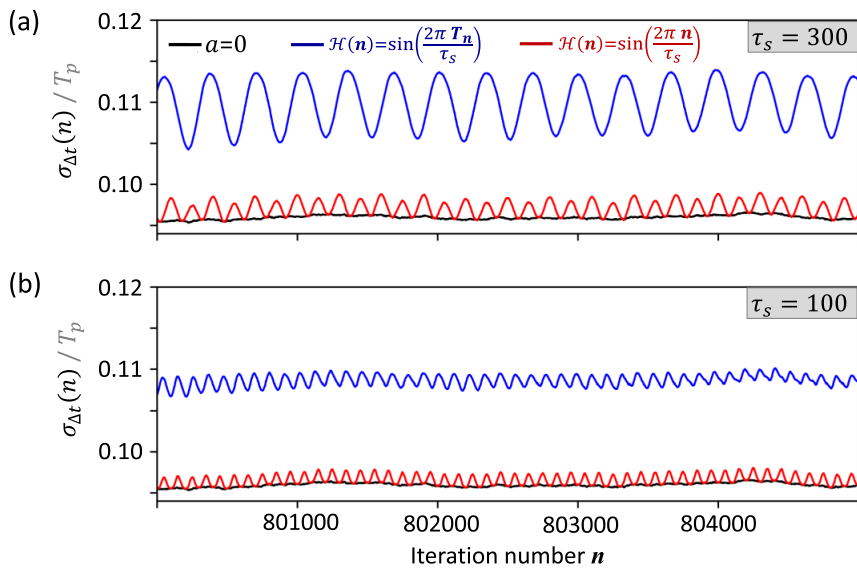


FIGURE 6. Jitter in a driven iterative map. Normalized standard deviation of the pulse arrival times $\sigma_{\Delta t}(n)$ as a function of the laser cavity roundtrip number as reproduced by the iterative map of (3.2): (a) $\tau_s=300$; (b) $\tau_s=100$. Black line shows the case of a random walk (no forcing function \mathcal{H}), blue and red lines show results with different driving terms \mathcal{H} (see legend). Parameters: $T_p = 1$.

in Figure 6, where the minima of the red line are on the black curve). If instead $\mathcal{H}(T_n) = \sin(2\pi T_n/\tau_s)$ is used, the added modulations do not cancel due to the fluctuations in the T_n values that enter the sine function, this leads to an overall increase in the variance (Figure 6, blue line). The mode-locked laser with feedback is comparable to the latter case as the noise-induced modulations are not perfectly periodic.

3.3. Optimized timing jitter reduction via dual-cavity feedback In the previous section, we have shown that noise-induced modulations are detrimental to the regularity of the pulse trains produced by passively mode-locked lasers. In this section, we investigate the influence of a second feedback cavity on the suppression of the noise-induced modulations and hence on the improvement of the timing regularity of the mode-locked laser output.

Noise-induced modulations are excitations of eigenmodes of a system which are only weakly damped. To ascertain the relative magnitude of the modulations, one looks at the eigenvalues of the underlying deterministic system. It has been shown that for oscillatory systems with delay, as, for example, the mode-locked laser subject to resonant feedback from two external cavities, the eigenvalues λ can be estimated by the solution of the characteristic equation given in (3.4) as a function of the two resonant delay times τ_1 and τ_2 [24]:

$$\lambda = -(K_1^{\text{eff}} + K_2^{\text{eff}}) + K_1^{\text{eff}} e^{-\lambda\tau_1} + K_2^{\text{eff}} e^{-\lambda\tau_2}. \quad (3.4)$$

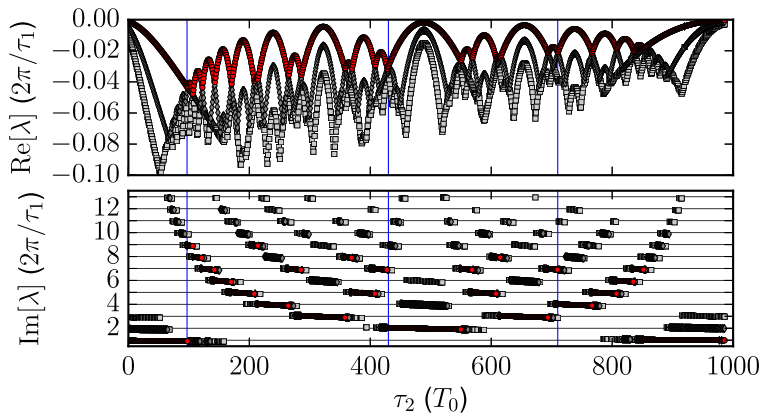


FIGURE 7. Real and imaginary parts of the largest eigenmodes of a passively mode-locked laser subject to feedback from two external cavities predicted from the fitted characteristic equation (3.4) [24]. Parameters: $K_1^{\text{eff}} = K_2^{\text{eff}} = 0.047$, $\tau_1 = 1000T_0$.

Differences between different oscillatory systems only occur in how strongly the feedback acts upon the system (via the effective feedback strengths $K_{1,2}^{\text{eff}}$), but not in the form of the characteristic equation [24]. Therefore, K_1^{eff} and K_2^{eff} can be determined numerically via fitting results for small delays to (3.4). We are interested in the influence of the length of the second feedback cavity, and hence, in Figure 7, the real and imaginary parts of the three largest eigenvalues are plotted as a function of τ_2 for $\tau_1 = 1000T_0$. The real part gives the damping rate of perturbations and the imaginary part gives the frequency of modulations that are excited by perturbations. This means that the smaller the real parts of the eigenvalues, the smaller the amplitude of the noise-induced modulations will be. For the case at hand, the largest damping rate occurs for $\tau_2 = 97T_0$.

In Figure 8, power spectra of the electric field amplitude are shown for the three τ_2 values marked by the blue vertical lines in Figure 7. These spectra show a significant suppression of the noise-induced modulations with respect to the single feedback cavity case (dark blue line). As predicted from the eigenvalues, the greatest suppression is achieved for $\tau_2 = 97T_0$. In addition to the reduction in the amplitude of the noise-induced modulations (indicated by the lower power in the side peaks of the power spectra), the dominant frequency of the modulations is also changed.

To make a fair comparison to the single feedback cavity case, the total feedback strength is kept the same, that is, $K_1 + K_2 = K$. This means that there is a trade off between oscillation suppression and long-term jitter reduction. The semi-analytic analysis in [23] showed that in the absence of noise-induced modulations, the long-term timing jitter decreases with increasing resonant feedback lengths according to (2.6). Therefore, if τ_2 is shorter, the contribution to this effect is reduced. However, the greatest oscillation suppression is expected for a relatively short second feedback cavity and the analysis of the previous section has shown that the noise-induced

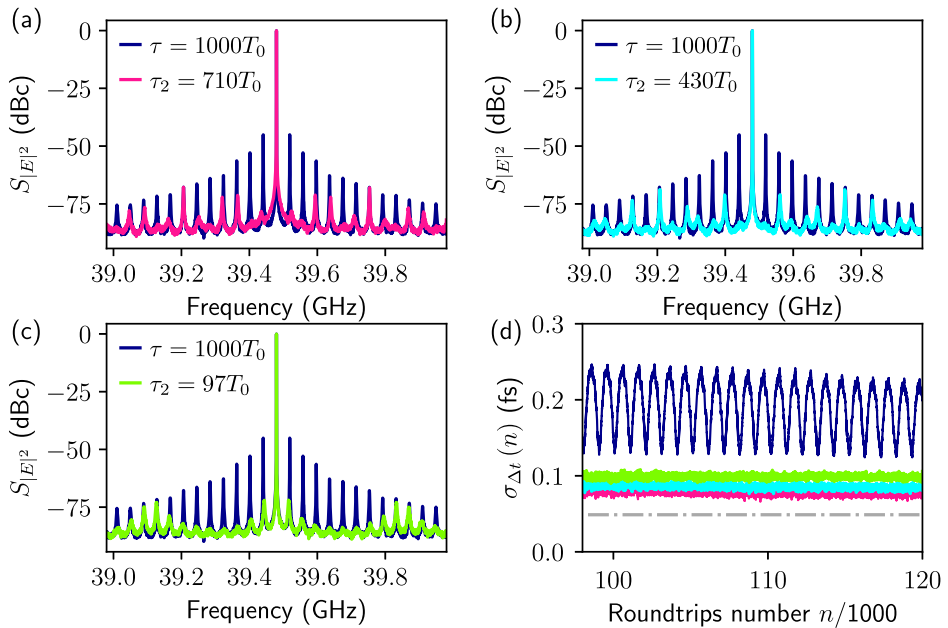


FIGURE 8. (a)–(c) Power spectra of the electric field $S_{|E|^2}$ and timing fluctuations $S_{|\Delta t_n|}$ of a passively mode-locked laser subject to feedback from two external cavities for delays indicated by the vertical blue lines in Figure 7. Blue lines show spectra for the $\tau = 1000T_0$ single feedback cavity case, while overlaid coloured spectra result from two delays. (d) Timing jitter $\sigma_{\Delta t}$, (3.1), for the case of one delay (blue) and two delays (colours as in the spectra in panels (a)–(c)), grey dashed line shows the long-term timing jitter. Parameters: $K = 0.1$, $K_1 = K_2 = 0.05$, $\tau_1 = 1000T_0$, all other parameters as in Table 1.

modulations cause the long-term jitter to increase. To determine the relative influence of these competing effects $\sigma_{\Delta t}(n)$ is plotted in Figure 8(d) for the single feedback case (dark blue) and the three dual feedback cases corresponding to Figure 8(a)–(c) (coloured). In all three dual feedback cases, it can clearly be seen that the modulations are suppressed. The long-term timing jitter is slightly different in the three cases, but in each case, it is lower than in the single feedback system. The best results are achieved for $\tau_2 = 710T_0$. For this feedback configuration, the long-term timing jitter is reduced by $\approx 40\%$ compared with the single feedback case, and the modulation of the timing fluctuations is effectively suppressed. Although the change in the long-term jitter is not very large, the reduction in the modulation amplitude represents a significant improvement in the regularity of the pulse train. For larger τ_2 values, the increase in the amplitude of the noise-induced modulations outweighs the influence of the longer cavity and the long-term timing jitter increases.

Experimentally, dual feedback configurations have been implemented and, although the delay lengths were not optimized, these studies showed a significant improvement in the r.m.s. timing jitter [5, 12, 19, 22]. In these works, the reduction in the r.m.s. timing jitter was larger than the reduction in the long-term jitter demonstrated numerical

here. This is expected due to the delay lengths used in these experimental studies. In [22], the delay length of the longer feedback cavity is approximately 3000 times the interspike interval time. For longer delay times, the amplitude of the noise-induced modulations is increased, which causes a greater increase in the variance of the timing fluctuations, and hence in the r.m.s. and long-term jitter, meaning that comparatively, a greater improvement can be achieved with a dual feedback setup.

4. Discussion and conclusions

We have shown how noise-induced modulation of the interspike intervals affects the timing regularity of passively mode-locked lasers subject to optical feedback. Although the occurrence of noise-induced modulations in such systems has been observed experimentally [3, 9, 47], so far, their influence has been neglected or has not been fully taken into account. The results presented here show that this can lead to large over estimates of the regularity of the emitted pulse trains. This is because the long-term timing jitter only gives an indication of the regularity of pulse trains over very long times and contains no information on fluctuations on shorter time scales. When the delay lengths are very long, then noise-induced fluctuations, which occur on the time scale of the feedback delay time, can cause larger variations in the pulse arrival times than the underlying random-walk-like drift. This effect becomes more important the longer the feedback cavity, as the damping rate of the noise-induced modulations decreases.

A significant improvement in the regularity of the emitted pulse trains can be achieved by adding a second feedback cavity of the appropriate length. This improvement occurs due to the suppression of the noise-induced modulations caused by an increase in the damping rate of the largest eigenmodes of the system. To find the optimal length for the second feedback cavity, minima in the largest eigenvalue need to be found. The eigenvalues depend on the feedback delay times and feedback strengths, and as such, the minima are not given by fixed ratios of τ_1 and τ_2 [24]. Generally, though, due to the trade off between oscillation suppression and the increased long-term timing jitter reduction achieved for longer delay times [23], the second delay length should be approximately three quarters the length of the first cavity.

By implementing a dual feedback configuration, the timing stability of a passively mode-locked laser can be substantially improved, making them promising devices for a wide range of applications.

References

- [1] G. P. Agrawal and N. K. Dutta, *Semiconductor lasers* (Van Nostrand Reinhold, New York, 1993); doi:10.1007/978-1-4613-0481-4.
- [2] R. Arkhipov, A. S. Pimenov, M. Radziunas, D. Rachinskii, A. G. Vladimirov, D. Arsenijević, H. Schmeckeber and D. Bimberg, "Hybrid mode locking in semiconductor lasers: simulations, analysis, and experiments", *IEEE J. Sel. Top. Quantum Electron.* **19** (2013) Article ID: 1100208; doi:10.1109/jstqe.2012.2228633.

- [3] D. Arsenijević, M. Kleinert and D. Bimberg, “Phase noise and jitter reduction by optical feedback on passively mode-locked quantum-dot lasers”, *Appl. Phys. Lett.* **103** (2013) Article ID: 231101; doi:[10.1063/1.4837716](https://doi.org/10.1063/1.4837716).
- [4] H. Asghar and J. G. McInerney, “Asymmetric dual-loop feedback to suppress spurious tones and reduce timing jitter in self-mode-locked quantum-dash lasers emitting at 1.55 μm ”, *Opt. Lett.* **42** (2017) 3714–3717; doi:[10.1364/ol.42.003714](https://doi.org/10.1364/ol.42.003714).
- [5] H. Asghar, W. Wei, P. Kumar, E. Sooudi and J. G. McInerney, “Stabilization of self-mode-locked quantum dash lasers by symmetric dual-loop optical feedback”, *Opt. Express* **26** (2018) 4581–4592; doi:[10.1364/oe.26.004581](https://doi.org/10.1364/oe.26.004581).
- [6] E. A. Avrutin, J. H. Marsh and E. L. Portnoi, “Monolithic and multi-gigahertz mode-locked semiconductor lasers: constructions, experiments, models and applications”, *IEE Proc. Optoelectron.* **147** (2000) Article ID: 251; doi:[10.1049/ip-opt:20000282](https://doi.org/10.1049/ip-opt:20000282).
- [7] E. A. Avrutin and B. M. Russell, “Dynamics and spectra of monolithic mode-locked laser diodes under external optical feedback”, *IEEE J. Quantum Electron.* **45** (2009) Article ID: 1456; doi:[10.1109/JQE.2009.2028242](https://doi.org/10.1109/JQE.2009.2028242).
- [8] A. G. Balanov, N. B. Janson and E. Schöll, “Control of noise-induced oscillations by delayed feedback”, *Phys. D* **199** (2004) 1–12; doi:[10.1016/j.physd.2004.05.008](https://doi.org/10.1016/j.physd.2004.05.008).
- [9] S. Breuer, W. Elsässer, J. G. McInerney, K. Yvind, J. Pozo, E. A. J. M. Bente, M. Yousefi, A. Villafranca, N. Vogiatzis and J. Rorison, “Investigations of repetition rate stability of a mode-locked quantum dot semiconductor laser in an auxiliary optical fiber cavity”, *IEEE J. Quantum Electron.* **46** (2010) 150; doi:[10.1109/jqe.2009.2033255](https://doi.org/10.1109/jqe.2009.2033255).
- [10] B. Dong, X. C. de Labriolle, S. Yu, M. Dumont, H. Huang, J. Duan, J. Norman, J. E. Bowers and F. Grillot, “1.3- μm passively mode-locked quantum dot lasers epitaxially grown on silicon: gain properties and optical feedback stabilization”, *J. Phys. Photonics* **2** (2020) Article ID: 045006; doi:[10.1088/2515-7647/aba5a6](https://doi.org/10.1088/2515-7647/aba5a6).
- [11] A. W. Drake, *Fundamentals of applied probability theory*, Probability and Statistics. McGraw-Hill Classic Textbook Reissue Series (McGraw-Hill, New York, 1967); <https://books.google.com.au/books?id=FhnvAAAAMAAJ>.
- [12] L. Drzewietzki, S. Breuer and W. Elsässer, “Timing jitter reduction of passively mode-locked semiconductor lasers by self- and external-injection: numerical description and experiments”, *Opt. Express* **21** (2013) 16142–16161; doi:[10.1364/oe.21.016142](https://doi.org/10.1364/oe.21.016142).
- [13] L. Drzewietzki, S. Breuer and W. Elsässer, “Timing phase noise reduction of modelocked quantum-dot lasers by time-delayed optoelectronic feedback”, *Electron. Lett.* **49** (2013) 557–559; doi:[10.1049/el.2013.0763](https://doi.org/10.1049/el.2013.0763).
- [14] M. Duque Gijón, A. Quirce, J. Tiana-Alsina, C. Masoller and Á. Valle, “Timing jitter reduction in semiconductor lasers induced by optical injection”, *Opt. Lett.* **48** (2023) 5655–5658; doi:[10.1364/ol.506152](https://doi.org/10.1364/ol.506152).
- [15] G. Fiol, D. Arsenijević, D. Bimberg, A. G. Vladimirov, M. Wolfrum, E. A. Viktorov and P. Mandel, “Hybrid mode-locking in a 40GHz monolithic quantum dot laser”, *Appl. Phys. Lett.* **96** (2010) Article ID: 011104; doi:[10.1063/1.3279136](https://doi.org/10.1063/1.3279136).
- [16] V. Flunkert and E. Schöll, “Suppressing noise-induced intensity pulsations in semiconductor lasers by means of time-delayed feedback”, *Phys. Rev. E* **76** (2007) Article ID: 066202; doi:[10.1103/physreve.76.066202](https://doi.org/10.1103/physreve.76.066202).
- [17] J. García-Ojalvo, M. B. Elowitz and S. H. Strogatz, “Modeling a synthetic multicellular clock: repressilators coupled by quorum sensing”, *Proc. Natl. Acad. Sci.* **101** (2004) 10955–10960; doi:[10.1073/pnas.0307095101](https://doi.org/10.1073/pnas.0307095101).
- [18] D. S. Goldobin, M. Rosenblum and A. Pikovsky, “Controlling oscillator coherence by delayed feedback”, *Phys. Rev. E* **67** (2003) Article ID: 061119; doi:[10.1103/PhysRevE.67.061119](https://doi.org/10.1103/PhysRevE.67.061119).
- [19] M. Haji, L. Hou, A. E. Kelly, J. Akbar, J. H. Marsh, J. M. Arnold and C. N. Ironside, “High frequency optoelectronic oscillators based on the optical feedback of semiconductor mode-locked laser diodes”, *Opt. Express* **20** (2012) 3268–3274; doi:[10.1364/oe.20.003268](https://doi.org/10.1364/oe.20.003268).

- [20] L. C. Jaurigue, *Passively mode-locked semiconductor lasers: dynamics and stochastic properties in the presence of optical feedback*, Springer thesis edition (Springer, Cham, 2017); doi:[10.1007/978-3-319-58874-2](https://doi.org/10.1007/978-3-319-58874-2).
- [21] L. C. Jaurigue, B. Krauskopf and K. Lüdge, “Multipulse dynamics of a passively mode-locked semiconductor laser with delayed optical feedback”, *Chaos* **27** (2017) Article ID: 114301; doi:[10.1063/1.5006743](https://doi.org/10.1063/1.5006743).
- [22] L. C. Jaurigue, O. Nikiforov, E. Schöll, S. Breuer and K. Lüdge, “Dynamics of a passively mode-locked semiconductor laser subject to dual-cavity optical feedback”, *Phys. Rev. E* **93** (2016) Article ID: 022205; doi:[10.1103/physreve.93.022205](https://doi.org/10.1103/physreve.93.022205).
- [23] L. C. Jaurigue, A. S. Pimenov, D. Rachinskii, E. Schöll, K. Lüdge and A. G. Vladimirov, “Timing jitter of passively mode-locked semiconductor lasers subject to optical feedback; a semi-analytic approach”, *Phys. Rev. A* **92** (2015) Article ID: 053807; doi:[10.1103/physreva.92.053807](https://doi.org/10.1103/physreva.92.053807).
- [24] L. C. Jaurigue, E. Schöll and K. Lüdge, “Suppression of noise-induced modulations in multidelay systems”, *Phys. Rev. Lett.* **117** (2016) Article ID: 154101; doi:[10.1103/physrevlett.117.154101](https://doi.org/10.1103/physrevlett.117.154101).
- [25] F. Kefelian, S. O’Donoghue, M. T. Todaro, J. G. McInerney and G. Huyet, “RF linewidth in monolithic passively mode-locked semiconductor laser”, *IEEE Photon. Technol. Lett.* **20** (2008) Article ID: 1405; doi:[10.1109/lpt.2008.926834](https://doi.org/10.1109/lpt.2008.926834).
- [26] D. C. Lee, “Analysis of jitter in phase-locked loops”, *IEEE Trans. Circuits Syst. II* **49** (2002) 704–711; doi:[10.1109/tcsii.2002.807265](https://doi.org/10.1109/tcsii.2002.807265).
- [27] F. Lelarge et al., “Recent advances on InAs/InP quantum dash based semiconductor lasers and optical amplifiers operating at $1.55\mu\text{m}$ ”, *IEEE J. Sel. Top. Quantum Electron.* **13** (2007) Article ID: 111; doi:[10.1109/jstqe.2006.887154](https://doi.org/10.1109/jstqe.2006.887154).
- [28] X. Li et al., “Phase noise reduction of a $2\mu\text{m}$ passively mode-locked laser through hybrid III-V/silicon integration”, *Optica* **8** (2021) 855–860; doi:[10.1364/optica.416007](https://doi.org/10.1364/optica.416007).
- [29] C. Y. Lin, F. Grillot, N. A. Naderi, Y. Yu and L. F. Lester, “RF linewidth reduction in a quantum dot passively mode-locked laser subject to external optical feedback”, *Appl. Phys. Lett.* **96** (2010) Article ID: 051118; doi:[10.1063/1.3299714](https://doi.org/10.1063/1.3299714).
- [30] K. Lüdge, L. C. Jaurigue, B. Lingnau, S. Terrien and B. Krauskopf, “Semiconductor mode-locked laser with external feedback: emergence of multi-frequency pulse trains with an increasing number of modes”, *Eur. Phys. J. B* **92** (2019) Article ID: 89; doi:[10.1140/epjb/e2019-90662-4](https://doi.org/10.1140/epjb/e2019-90662-4).
- [31] K. Lüdge and E. Schöll, “Temperature dependent two-state lasing in quantum dot lasers”, in: *Laser dynamics and nonlinear photonics, fifth Rio De La Plata Workshop 6–9 Dec. 2011*, IEEE Conf. Proc. (IEEE Publishing Services, New York, 2012) 1–6; doi:[10.1109/ldnp.2011.6162081](https://doi.org/10.1109/ldnp.2011.6162081).
- [32] S. Meinecke and K. Lüdge, “Efficient timing jitter simulation for passively mode-locked semiconductor lasers”, *Appl. Phys. Lett.* **118** (2021) Article ID: 011104; doi:[10.1063/5.0036928](https://doi.org/10.1063/5.0036928).
- [33] O. Nikiforov, L. C. Jaurigue, L. Drzewietzki, K. Lüdge and S. Breuer, “Experimental demonstration of change of dynamical properties of a passively mode-locked semiconductor laser subject to dual optical feedback by dual full delay-range tuning”, *Opt. Express* **24** (2016) 14301–14310; doi:[10.1364/oe.24.014301](https://doi.org/10.1364/oe.24.014301).
- [34] C. Otto, *Dynamics of quantum dot lasers – effects of optical feedback and external optical injection*, Springer Theses (Springer, Heidelberg, 2014); doi:[10.1007/978-3-319-03786-8](https://doi.org/10.1007/978-3-319-03786-8).
- [35] C. Otto, B. Globisch, K. Lüdge, E. Schöll and T. Erneux, “Complex dynamics of semiconductor quantum dot lasers subject to delayed optical feedback”, *Int. J. Bifur. Chaos* **22** (2012) Article ID: 1250246; doi:[10.1142/s021812741250246x](https://doi.org/10.1142/s021812741250246x).
- [36] C. Otto, L. C. Jaurigue, E. Schöll and K. Lüdge, “Optimization of timing jitter reduction by optical feedback for a passively mode-locked laser”, *IEEE Photonics J.* **6** (2014) Article ID: 1501814; doi:[10.1109/jphot.2014.2352934](https://doi.org/10.1109/jphot.2014.2352934).
- [37] C. Otto, K. Lüdge, A. G. Vladimirov, M. Wolfrum and E. Schöll, “Delay induced dynamics and jitter reduction of passively mode-locked semiconductor laser subject to optical feedback”, *New J. Phys.* **14** (2012) Article ID: 113033; doi:[10.1088/1367-2630/14/11/113033](https://doi.org/10.1088/1367-2630/14/11/113033).

- [38] A. S. Pimenov, T. Habruseva, D. Rachinskii, S. P. Hegarty, G. Huyet and A. G. Vladimirov, “Effect of dynamical instability on timing jitter in passively mode-locked quantum-dot lasers”, *Opt. Lett.* **39** (2014) Article ID: 6815; doi:[10.1364/ol.39.006815](https://doi.org/10.1364/ol.39.006815).
- [39] A. S. Pimenov and A. G. Vladimirov, “Dynamics of an inhomogeneously broadened passively mode-locked laser”, *Eur. Phys. J. B* **92** (2019) Article ID: 114; doi:[10.1140/epjb/e2019-90642-8](https://doi.org/10.1140/epjb/e2019-90642-8).
- [40] O. Pottiez, O. Deparis, R. Kiyam, M. Haelterman, P. Emplit, P. Mégret and M. Blondel, “Supermode noise of harmonically mode-locked erbium fiber lasers with composite cavity”, *IEEE J. Quantum Electron.* **38** (2002) 252–259; doi:[10.1109/3.985565](https://doi.org/10.1109/3.985565).
- [41] E. U. Rafailov, M. A. Cataluna and W. Sibbett, “Mode-locked quantum-dot lasers”, *Nat. Photonics* **1** (2007) 395–401; doi:[10.1038/nphoton.2007.120](https://doi.org/10.1038/nphoton.2007.120).
- [42] N. Rebrova, T. Habruseva, G. Huyet and S. P. Hegarty, “Stabilization of a passively mode-locked laser by continuous wave optical injection”, *Appl. Phys. Lett.* **97** (2010) Article ID: 101105; doi:[10.1063/1.3483231](https://doi.org/10.1063/1.3483231).
- [43] N. Rebrova, G. Huyet, D. Rachinskii and A. G. Vladimirov, “Optically injected mode-locked laser”, *Phys. Rev. E* **83** (2011) Article ID: 066202; doi:[10.1103/physreve.83.066202](https://doi.org/10.1103/physreve.83.066202).
- [44] T. G. Seidel, J. Javaloyes and S. V. Gurevich, “Influence of time-delayed feedback on the dynamics of temporal localized structures in passively mode-locked semiconductor lasers”, *Chaos* **32** (2022) Article ID: 033102; doi:[10.1063/5.0075449](https://doi.org/10.1063/5.0075449).
- [45] D. Sigeti and W. Horsthemke, “Pseudo-regular oscillations induced by external noise”, *J. Stat. Phys.* **54** (1989) Article ID: 1217; doi:[10.1007/BF01044713](https://doi.org/10.1007/BF01044713).
- [46] C. Simos, H. Simos, C. Mesaritakis, A. Kapsalis and D. Syvridis, “Pulse and noise properties of a two section passively mode-locked quantum dot laser under long delay feedback”, *Opt. Commun.* **313** (2014) 248–255; doi:[10.1016/j.optcom.2013.10.034](https://doi.org/10.1016/j.optcom.2013.10.034).
- [47] O. Solgaard and K. Y. Lau, “Optical feedback stabilization of the intensity oscillations in ultrahigh-frequency passively modelocked monolithic quantum-well lasers”, *IEEE Photon. Technol. Lett.* **5** (1993) Article ID: 1264; doi:[10.1109/68.250039](https://doi.org/10.1109/68.250039).
- [48] A. G. Vladimirov, U. Bandelow, G. Fiol, D. Arsenijević, M. Kleinert, D. Bimberg, A. S. Pimenov and D. Rachinskii, “Dynamical regimes in a monolithic passively mode-locked quantum dot laser”, *J. Opt. Soc. Am. B* **27** (2010) Article ID: 2102; doi:[10.1364/josab.27.002102](https://doi.org/10.1364/josab.27.002102).
- [49] A. G. Vladimirov and D. V. Turaev, “Model for passive mode locking in semiconductor lasers”, *Phys. Rev. A* **72** (2005) Article ID: 033808; doi:[10.1103/physreva.72.033808](https://doi.org/10.1103/physreva.72.033808).
- [50] A. G. Vladimirov, D. V. Turaev and G. Kozyreff, “Delay differential equations for mode-locked semiconductor lasers”, *Opt. Lett.* **29** (2004) Article ID: 1221; doi:[10.1364/ol.29.001221](https://doi.org/10.1364/ol.29.001221).
- [51] D. von der Linde, “Characterization of the noise in continuously operating mode-locked lasers”, *Appl. Phys. B* **39** (1986) Article ID: 201; doi:[10.1007/bf00697487](https://doi.org/10.1007/bf00697487).
- [52] H. Wang, L. Guo, W. Zhao, G. Chen, D. Lu and L. Zhao, “Reducing the RF linewidth and timing jitter of a mode-locked semiconductor laser using optical feedback scheme”, in: *2018 Asia communications and photonics conference (ACP)* (IEE Publishing Services, New York, 2018) 1–3; doi:[10.1109/acp.2018.8596174](https://doi.org/10.1109/acp.2018.8596174).
- [53] Z.-H. Wang, W.-Q. Wei, Q. Feng, T. Wang and J.-J. Zhang, “InAs/GaAs quantum dot single-section mode-locked lasers on Si (001) with optical self-injection feedback”, *Opt. Express* **29** (2021) 674–683; doi:[10.1364/oe.411551](https://doi.org/10.1364/oe.411551).
- [54] S. Yanchuk and P. Perlikowski, “Delay and periodicity”, *Phys. Rev. E* **79** (2009) Article ID: 046221; doi:[10.1103/physreve.79.046221](https://doi.org/10.1103/physreve.79.046221).
- [55] L. Zheng, R. Wang, T. Zhou and K. Aihara, “Noise-induced cooperative behavior in a multicell system”, *Bioinformatics* **21** (2005) 2722–2729; doi:[10.1093/bioinformatics/bti392](https://doi.org/10.1093/bioinformatics/bti392).